

Photocatalytic Degradation of Camphor by Suspended and Immobilized Photocatalysts

Carla Sirtori,^a Adriane M. de Freitas,^a Sérgio Toshio Fujiwara^b and Patricio Peralta-Zamora^{*a}

^aDepartamento de Química, Universidade Federal do Paraná, CP 19081, 81531-990 Curitiba-PR, Brazil

^bDepartamento de Química, Universidade Estadual do Centro-Oeste, Rua Simeão Camargo Varela de Sá, 03, 85040-080 Guarapuava-PR, Brazil

Neste trabalho, a degradação de cânfora em solução aquosa foi avaliada utilizando-se processos fotocatalíticos mediados por suspensões e formas imobilizadas de TiO₂ e ZnO. Os catalisadores suportados (TiO₂/anéis de vidro, TiO₂/alginato de cálcio e ZnO/alginato de cálcio) foram caracterizados por microscopia eletrônica de varredura com espectroscopia de energia dispersiva de raios X (SEM/EDX), difratometria de raios X (XRD), fluorescência de raios X por energia dispersiva (EDXRF) e espectroscopia Raman, técnicas que permitiram confirmar a elevada porosidade dos materiais, assim como as fases cristalinas características (anatase e wurtzita). A eficiência de degradação dos fotocatalisadores suportados foi comparada com a dos semicondutores em suspensão, observando-se resultados comparáveis entre TiO₂ Degussa P25 e TiO₂ imobilizado em anéis de vidro. Por outro lado, o uso de esferas de alginato de cálcio propiciou menores eficiências de degradação, provavelmente em decorrência da significativa redução da área superficial nos sistemas imobilizados.

In this work, the degradation of aqueous solution of camphor by heterogeneous photocatalysis was study using suspended and supported TiO₂ and ZnO. The supported catalysts (TiO₂/borosilicate reaching ring, TiO₂/calcium alginate and ZnO/calcium alginate) were characterized by scanning electron microscopy coupled with energy dispersive X-ray spectroscopy (SEM/EDX), X-ray diffractometry (XRD), energy dispersive X-ray fluorescence (EDXRF) and Raman spectroscopy, techniques that permitted to confirm the porosity of the material as well as the characteristic crystalline forms (anatase and wurtzite). The degradation efficiency of the supported photocatalysts was compared with the performance of free TiO₂ and ZnO, observing comparable results between conventional Degussa P25 TiO₂ and TiO₂ immobilized in glass-rings. On the other hand, the use of calcium alginate beads leads to lower degradation efficiency probably due to the significant area reduction observed in immobilized systems.

Keywords: camphor, photocatalysis, immobilized photocatalysts, TiO₂, ZnO

Introduction

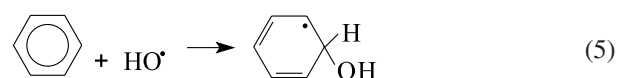
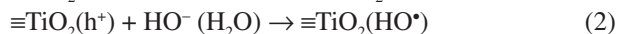
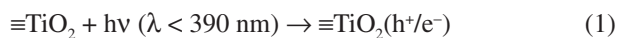
In the last decades, many works have demonstrated the high degradation capacity of heterogeneous photocatalysis, mainly with the use of titanium dioxide (TiO₂) as photocatalyst.¹ Interesting and complete revisions were recently published, remarking some important environmental applications.^{2,3} Many recalcitrant pollutants can be quickly degraded and mineralized by heterogeneous photocatalysis, usually with low influence of its chemical

nature.³ In view of this fact, photocatalysis has been successfully used for degradation of pesticides,⁴ polycyclic aromatic hydrocarbons,⁵ textile dyes,⁶ spill oils,⁷ among other substrates of environmental relevance.

Even involving complex reductive and oxidative mechanisms, favored by the high oxidant character of the positive hole ($E^0 = +2.53$ V vs. ENH) and the moderate reductive capacity of the electron ($E^0 = -0.52$ V vs. ENH), it is admitted that the main reaction mechanism is mediated by hydroxyl radical. This is a strong oxidant agent ($E^0 = +2.80$ V vs. ENH) that results from the reaction between the positive hole and hydroxyl ion (or water molecules)

*e-mail: zamora@ufpr.br

previously adsorbed onto the photocatalyst surface (equations 1-2). Usually, heterogeneous photocatalytic reactions mediated by hydroxyl radicals show velocity between 10^6 and 10^9 mol L⁻¹ s⁻¹.³ These mainly involve hydrogen abstraction in saturated organic compounds (equation 3), electron transference in neutral or charged inorganic compounds (equation 4) and radical addition in aromatic molecules (equation 5).



Even showing high degradation efficiency, the implementation of large-scale heterogeneous photocatalytic procedures represents a very difficult task, mainly in view of the difficult separation of nanometric photocatalysts at the end of the process.^{8,9} To overcome these difficulties, many immobilized photocatalysts have been proposed, involving the use of glass-rings (Raschig rings)¹⁰ and glass-tubes,¹¹ activated charcoal,⁸ silica,¹² among other support materials. In some situations, the use of immobilized photocatalysts reduces the efficiency of the degradation process, in view of the considerable reduction of disposable sites for adsorption and catalysis.¹³ In other conditions, the use of immobilized photocatalysts enhances the efficiency of the degradation process, mainly on account of the preliminary adsorption of the substrates onto the support surface. A fact that facilitates its approximation to the disposable catalytic sites.¹⁴

Several works have shown a superior degradation efficiency of photocatalytic systems mediated by ZnO.^{15,16} However, a small number of works related the use of immobilized forms of this photocatalyst, outstanding the good results observed by the use of ZnO immobilized in glass-rings¹⁰ and plates.¹⁷ As far as, it is known only one work that relates the use of ZnO immobilized into calcium alginate beads, with excellent degradation capacity of textile dyes in reaction times of about 120 min.¹⁸

In this work, the potentiality of immobilized forms of TiO₂ and ZnO was evaluated, toward the photocatalytic degradation of camphor in aqueous solution. Camphor was selected as a model substrate due to its close chemical similarity with 2-methylisoborneol (2-MIB). 2-MIB is one of the chemicals with major influence on the quality of drinking water, on account of its, very low odor detection threshold.¹⁹ The photocatalytic degradation of 2-MIB by

using TiO₂ supported on Y-zeolites was recently reported, with results that demonstrate the best degradation capacity of the immobilized photocatalyst, mainly in consequence of the preliminary adsorption of 2-MIB into the support material.²⁰

Experimental

Chemical and reagents

Camphor (Viafarma, 98%) was used in aqueous solutions of 50 mg L⁻¹. In heterogeneous photocatalytic processes, it was used titanium dioxide Degussa P-25 (75% anatase/25% rutile, BET 50 m² g⁻¹) and zinc oxide Merck (wurtzite, BET 4 m² g⁻¹). Immobilization studies involved the use of sodium alginate (Vetec, PA) and titanium (IV) butoxide (DuPont, 99%). In liquid-liquid extraction procedures, it was used dichloromethane (Vetec, PA). Other reagents were of analytical grade.

Immobilization of TiO₂ and ZnO in calcium alginate

The immobilizations of both photocatalysts were carried out according to procedures described by Rodríguez-Couto *et al.*¹⁸ A sodium alginate (3% m/v) solution was initially prepared in deionized water. Afterward, a suspension was prepared by using 1 L of sodium alginate and 1 g of photocatalyst (TiO₂ or ZnO). After thoroughly mixing, the calcium alginate beads were prepared by dropping the former suspension in an aqueous solution of calcium chloride (2%, m/m) with the aid of a peristaltic pump.

Immobilization of TiO₂ in borosilicate Raschig rings

The impregnation of TiO₂ in borosilicate Raschig rings was carried out according to procedures described by Yeber *et al.*²¹ Glass rings (5 × 2 mm) were left in contact for 45 min with a 5% (m/v) solution of titanium butoxide in ethanol. Afterward, the rings were calcinated at 450 °C for 45 min. The process was repeated by four times.

Characterization of the immobilized photocatalysts

The surface morphologies of the supported catalysts were evaluated by using scanning electron microscopy (SEM) in combination with energy dispersive X-ray analysis on a JEOL microscope operating at 20 keV. The X-ray powder diffraction (XRD) patterns were recorded on a Shimadzu XRD-6000 diffractometer using Cu K_α radiation (λ = 1.54 Å) operating at 40 kV, 20 mA and scanning rate of 2 degree min⁻¹. X-ray fluorescence

analyses (EDXRF) were carried on a Shimadzu-EDX 700 spectrometer. Raman spectra were obtained in a Renishaw Raman Image spectrophotometer coupled to an optical microscope that focuses the incident radiation down to a 1 mm spot. An Ar laser (514 nm) with an incident potency of 50% was used over the 200-1000 cm^{-1} region. UV-Vis spectra were recorded in a Shimadzu UV-2401 PC equipment, using 1 cm quartz cells.

Photocatalytic treatment

Photocatalytical experiments were carried out in a jacketed borosilicon-glass vessel (250 mL), equipped with magnetic stirrer, water refrigeration (operating temperature of 25 ± 2 °C) and oxygenation system (oxygen flow of 45 mL min^{-1}). The UV radiation was provided by a medium-pressure mercury vapor lamp (125 W, maximal emission wavelength centered at 254 nm), without the original glass-bulb, immersed in the samples by means of a quartz jacket. Under these conditions, the measured UV photon flux was 9.7×10^{-5} Einstein s^{-1} (uranyl-oxalate actinometry).

Samples of 250 mL were placed in the reactor and irradiated for different times, using a photocatalyst mass and a working pH previously optimized by factorial design. The pH value of the samples was adjusted with aqueous solutions of HNO_3 and NaOH . Samples were collected at regular intervals and submitted to analytical control.

To investigate the single effect of the adsorption on the photocatalyst surface, the degradation by photolysis and the removal by volatilization, experiments were carried out with suspensions of TiO_2 (or ZnO) in the dark, with single incidence of UV radiation and with single oxygenation (oxygen flow of 45 mL min^{-1}), respectively.

All experiments were carried out in triplicate, observing a mean relative standard deviation of approximately 3%.

Analytical control

The camphor degradation was monitored by gas chromatography with flame ionization detection (GC-FID) after extraction in dichloromethane. The chromatographic analysis was carried out in a Shimadzu 14B gas chromatographer, equipped with FID and a Shimadzu C-RGA area integrator. A 30 m \times 0.25 mm I.D., 0.25 μm film thickness DB-Wax (J & W Scientific) capillary column was used. Peak-area ratios between camphor and the internal standard (*n*-octanol) were used to construct a calibration curve over the range of 5-50 mg L^{-1} . The typical variance coefficient was 2.5%.

The total organic carbon (TOC) content was determined in a Shimadzu VCPH TOC analyzer. The calibration curve was made from a standard aqueous solution of potassium hydrogen phthalate over the range 5-200 mg L^{-1} . The typical variance coefficient was 2.0%.

Result and Discussions

Preliminary studies

Initially, the effect of relevant operational variables (pH and photocatalyst concentration) in the degradation capacity of the photocatalytic process was evaluated by a 2^2 factorial design, using suspended TiO_2 . For a better visualization, the results are shown as geometric representations in Figure 1, using the degradation of camphor at a reaction time of 60 min as analytical response. In both designs, a central point was assayed in triplicate, showing a mean standard deviation (SD) of 2%.

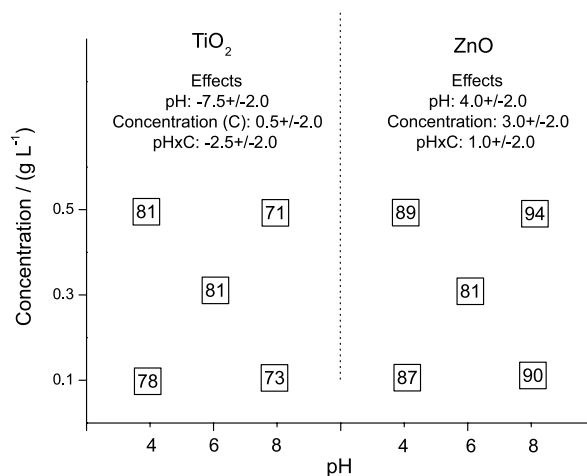


Figure 1. Geometric representation of the 2^2 factorial design used to evaluate the effect of pH and photocatalyst concentration on the degradation of camphor by suspended TiO_2 (camphor: 50 mg L^{-1} , reaction time: 15 min, monitoring: gas chromatography).

For TiO_2 (Figure 1), changes on the photocatalyst concentration (0.1 to 0.5 g L^{-1}) do not induce significant modification on the degradation capacity of the system, a fact that can be corroborated by a main effect (0.5%) lower than the SD value (2%). On the other hand, pH shows a negative main effect (-7.5%), which implies a higher degradation capacity in pH values near to the inferior level (4.0). The interpretation of the pH effect is always a difficult task mainly due to its significant influence on the chemical structure of the substrate and in the superficial properties of the photocatalyst. TiO_2 shows a zero-charge point at pH 6, a fact that implies a positively charged surface at pH lower than 6. Under these conditions, the migration

of photo-generated electrons is favored, a fact that reduces the electron-hole combination and consequently improves the efficiency of the photochemical process.²²

In studies involving the use of ZnO (Figure 1), effects of relevance were not observed. However, a slightly improved degradation capacity was observed at pH 8, provably on account of the negative effect provoked by the dissolution of ZnO in acidic media.

In view of the preceding observations, the concentration of photocatalysts were fixed in 0.2 g L⁻¹ and pH in 5.2, value that represents the natural pH of camphor aqueous solutions.

Because of the peculiar nature of the photocatalytic processes, the removal of camphor can be a result of some simultaneous processes, highlighting the adsorption on the photocatalyst surface, the losses by volatilization and the decomposition by photolytic degradation. In consequence, the single contribution of these processes was investigated, observing the results shown in Figure 2. Firstly, it is important to remark that, even when the preliminary adsorption of the substrates corresponds to an important condition for its photocatalytic degradation, the adsorption removal of camphor was not significant (< 10%), mainly taking into account the removal by photocatalysis (> 90%). Furthermore, it is possible to observe a higher adsorption capacity of TiO₂ probably due to its higher superficial area.

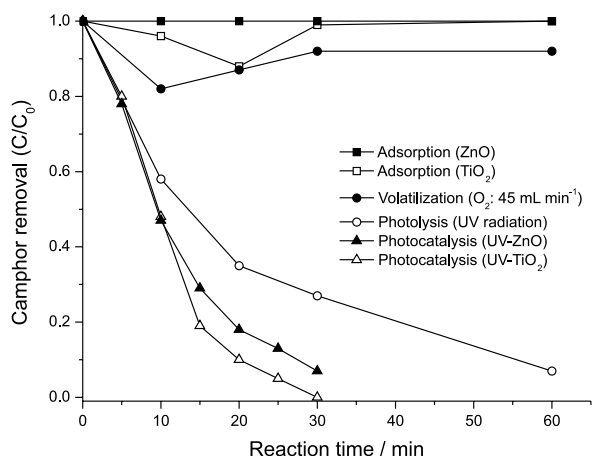


Figure 2. Removal of camphor by adsorption (TiO₂ or ZnO suspensions in the dark), volatilization by oxygenation (O₂: 45 mL min⁻¹), UV photolysis (single incidence of UV radiation) and heterogeneous photocatalysis (TiO₂ or ZnO suspensions under irradiation). Camphor: 50 mg L⁻¹, pH: 5.2, photocatalyst: 0.2 g L⁻¹, monitoring: gas chromatography.

Under the experimental conditions of this study (oxygen flow of 45 mL min⁻¹), the removal of camphor by volatilization was lower than 20%.

The effect of the single photolysis needs to be emphasized, by reason of degradation ratios of about 70% at reaction times of 30 min. Usually, the photolytic

process involves the scission of more labile bonds, without expressive mineralization.²³ In this study, the photolysis induced total organic carbon (TOC) removal lower than 20%. While in photocatalytic processes, the TOC removal was higher than 50% (ZnO) and 85% (TiO₂), at reaction times of 60 min.

The photocatalysis mediated by both semiconductors permits fast camphor degradation with practically complete removal at reaction times of 30 (TiO₂) and 45 min (ZnO).

Immobilization of TiO₂ and ZnO in calcium alginate

Alginate is a water soluble linear polysaccharide extracted from brown seaweed, containing alternating blocks of 1-4-linked α -L-guluronic and β -D-mannuronic acid residues. The most important property of alginates is their ability to form gels by reaction with divalent cations such as Ca²⁺.²⁴ The gelation and cross-linking of the polymers lead to formation of a characteristic egg-box structure, which permits the encapsulation of many chemical species.²⁵

In this work, ZnO and TiO₂ were incorporated into the calcium alginate beads by mean of a very simple procedure, which permits the formation of regular spheres with average diameter of 2-3 mm. Characterization studies carried out by scanning electronic microscopy permitted the observation of a very irregular surface with diverse pore dimensions. The chemical mapping evidenced a homogeneous distribution of both photocatalyst into the bead surface (Figure 3).

The concentration of the photocatalysts in the alginate beads were determined by X-ray fluorescence spectrometry with results of about 0.4% (m/m) for both semiconductors. Characterization studies carried out by Raman spectroscopy do not reveal significant details mainly due to the severe interference from the support fluorescence.

The characterization by X-ray diffractometry (XRD) evidenced the amorphous nature of the calcium alginate, feature that makes difficulty the identification of the crystalline phases of TiO₂. Anatase and rutile phases were observed in the step diffractogram acquired under reduced scanning velocity. In the characterization of alginate/ZnO, only one crystalline form of ZnO was evident. Moreover, it can be observed that, as presupposed, the phases of both oxides were not modified during the sample preparation, mainly in view of the mild used drying process (Figure 4).

Immobilization of TiO₂ in glass rings

Many works report the efficient immobilization of TiO₂ in glass supports, mainly by sol-gel processes involving the use of alcoxide precursors.²⁶

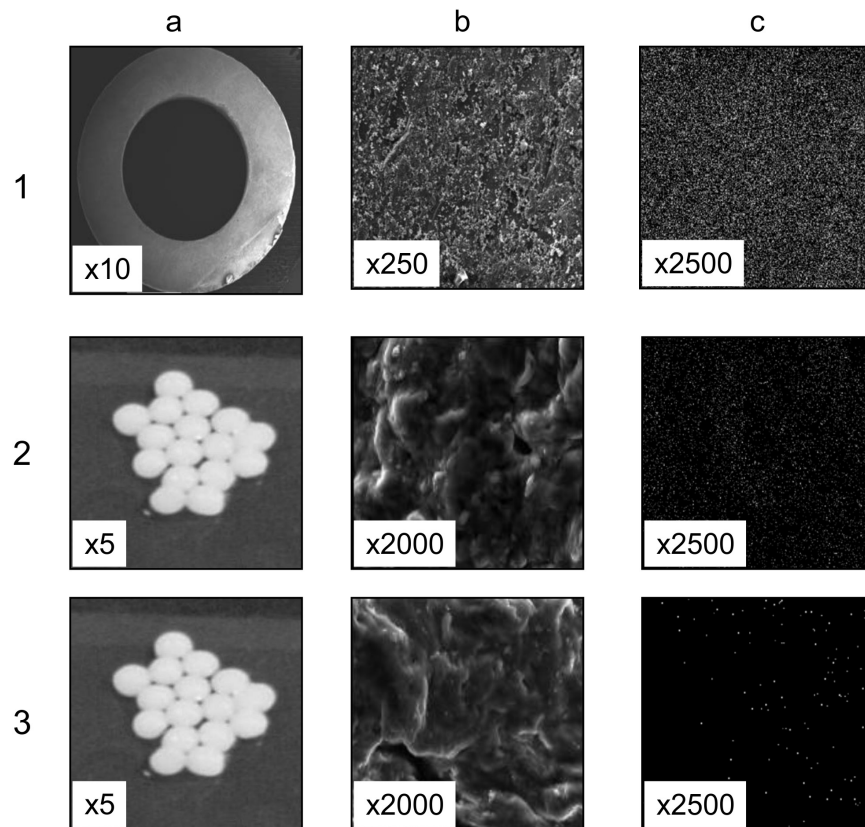


Figure 3. Electronic micrographs (a and b) and chemical mapping (c) of TiO₂/borosilicate reaching rings (1), TiO₂/Alginate (2) and ZnO/Alginate (3).

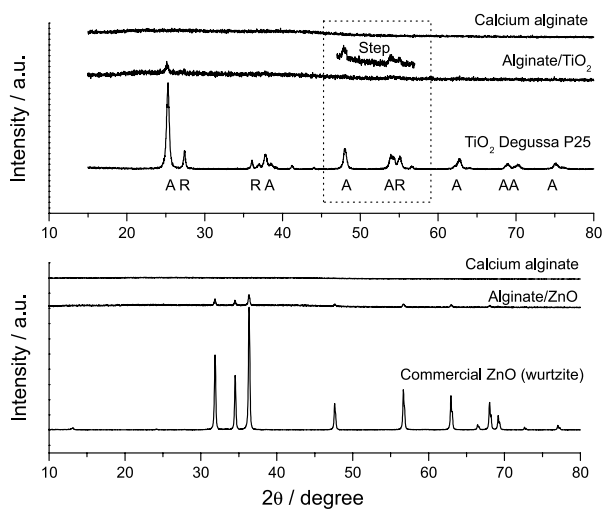


Figure 4. XRD patterns of calcium alginate and supported photocatalysts.

In this work, the XRD characterization did not revealed any crystalline phase of TiO₂, but only the presence of an amorphous solid (borosilicate glass), while the X-ray fluorescence analysis showed a TiO₂ concentration of about 15% (m/m). The UV spectra (Figure 5) showed a high similarity between the commercial Degussa P25 TiO₂ and the supported form, with a slight absorption edge shifts toward higher wavelengths, probably

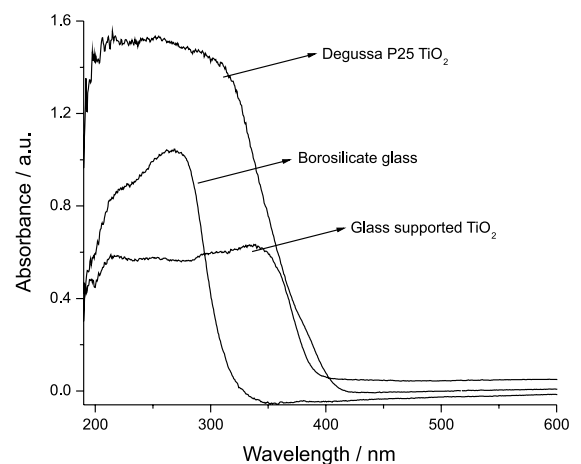


Figure 5. Electronic spectra of borosilicate glass, Degussa P25 TiO₂ and TiO₂ immobilized in borosilicate reaching rings.

on account of interactions between TiO₂ and the glass support.²⁷

Raman spectroscopy analysis (Figure 6) reveals the presence of bands in 396, 514 and 636 cm⁻¹, attributed to the B_{1g}, A_{1g} + B_{1g} and E_g anatase active modes.²⁸

Characterization studies carried out by scanning electronic microscopy and chemical mapping evidenced a homogeneous distribution of TiO₂ into the ring surface (Figure 3).

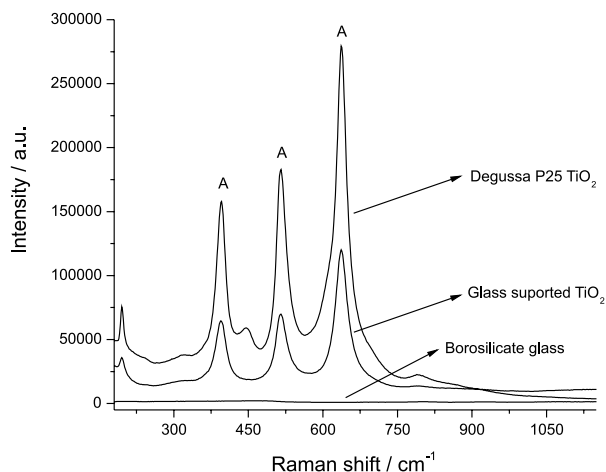


Figure 6. Raman spectra of borosilicate glass, Degussa P25 TiO₂ and TiO₂ immobilized in borosilicate reaching rings.

Degradation studies with suspended and supported photocatalysts

After characterization, the efficiency of the immobilized material was evaluated toward the degradation of camphor aqueous solutions, with the same experimental conditions used in degradation studies involving suspended photocatalysts (pH of camphor solution ca. 5.2 and 0.2 g L⁻¹ of semiconductor mass).

In order to quantitatively compare the processes, kinetic parameters were calculated from the degradation profiles shown in Figure 7.

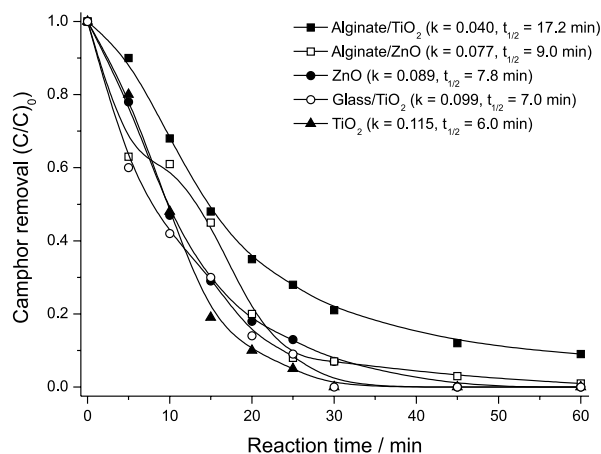


Figure 7. Degradation of camphor by photocatalysis using free and immobilized photocatalysts (camphor: 50 mg L⁻¹, pH: 5.2, photocatalyst: 0.2 g L⁻¹, monitoring: gas chromatography).

Because of its heterogeneous character, the kinetics of the photocatalytic processes generally follows a Langmuir-Hinshelwood mechanism, defined as:

$$r = k\theta = k(KC/(1 + KC))$$

where k is the true rate constant, K is the constant of adsorption at equilibrium and C is the instantaneous concentration.

For diluted solutions, KC becomes $\lll 1$. For this reason, the photocatalytic degradation of many organics substrates obeys apparently pseudo-first order kinetics at low initial substrate concentrations.

In this work, the *quasi*-exponential decay observed during the photocatalytic degradation of camphor, the linear relation observed between $\ln(C/C_0)$ and the reaction time indicate that, in our experimental conditions, the camphor degradation follows a pseudo-first order kinetic, as admitted in several works of similar nature.²⁹

For ZnO (Figure 7), very similar results were observed in supported ($k = 0.077$, $t_{1/2} = 9.0$ min) and unsupported ($k = 0.089$, $t_{1/2} = 7.5$ min) systems, a fact that implies almost total removal of camphor in reaction times of about 60 min. During the photocatalytic treatment, a slight decomposition of the alginate matrix was observed, a fact that provokes an also slight increase on the soluble TOC content. For this reason, it was not possible to assess de camphor mineralization.

The use of TiO₂ immobilized in borosilicate rings allowed degradation rates that are fairly similar to those observed with the use of suspensions of TiO₂ (Figure 7). That is, nearly complete degradation in reaction times of about 45 min. However, the mineralization was significantly different. The use of suspensions of TiO₂ allowed reduction of about 80% in the TOC content in reaction times of 60 min, whereas immobilized system induced mineralization not superior to 50%.

On the other hand, the degradation capacity of TiO₂ immobilized in alginate ($k = 0.040$, $t_{1/2} = 17.2$ min) was significantly lower than that observed with the use of TiO₂ suspensions ($k = 0.115$, $t_{1/2} = 6.0$ min) probably due to the significant area reduction observed in immobilized systems.

Unfortunately, few works have reported the photocatalytic degradation of 2-MIB. In general, the results reported here are comparable with that related in the current literature for photocatalytic degradation of 2-MIB by suspensions of TiO₂.¹⁹ On the other hand, the use of TiO₂ immobilized in glass-rings shows a better degradation performance than other immobilized forms, such as TiO₂/zeolites.²⁰

Conclusions

First of all, it is important to remark that high degradation efficiency was observed in photocatalytic processes assisted by free ZnO, in general with results that are comparable with those provided by TiO₂.

The degradation efficiency of TiO₂ supported in reaching glass ring was also comparable with the performance of free conventional Degussa P25 TiO₂. In both cases, almost total camphor removal was observed at reaction time lower than 60 min.

The use of calcium alginate beads as immobilization matrix show some inconveniences, mainly represented by low degradation efficiency when compared with free photocatalysts and instability under photochemical reactions, a fact that induced losses of soluble total organic carbon.

References

- Fujishima, A.; Rao, T. N.; Tryk, D. A.; *J. Photochem. Photobiol., C* **2000**, *1*, 1.
- Fujishima, A.; Zhang, X.; Tryk, D. A.; *Int. J. Hydrogen Energy* **2007**, *32*, 2664.
- Malato, S.; Fernández-Ibáñez, P.; Maldonado, M. I.; Blanco, J.; Gernjak, W.; *Catal. Today* **2009**, *147*, 1.
- Devipriya S.; Yesodharan, S.; *Sol Energy Mater. Sol. Cells* **2005**, *86*, 309.
- Woo, O. T.; Chung, W. K.; Wong, K. H.; Chow, A. T.; Wong, P. K.; *J. Hazard Mater.* **2009**, *168*, 1192.
- Zayani, G.; Bousselmi, L.; Mhenni, F.; Ghrabi, A.; *Desalination* **2009**, *246*, 344.
- Hsu, Y.-Y.; Hsiung, T.-L.; Wang, H.P.; Fukushima, Y.; Wei, Y.-L.; Chang, J.-E.; *Mar. Pollut. Bull.* **2008**, *57*, 873.
- Wang, X.; Liu, Y.; Hu, Z.; Chen, Y.; Liu, W.; Zhao, G.; *J. Hazard Mater.* **2009**, *169*, 1061.
- Khataee, A. R.; Pons, M. N.; Zahraa, O.; *J. Hazard Mater.* **2009**, *168*, 451.
- Yeber, M. C.; Rodríguez, J.; Freer, J.; Durán, N.; Mansilla, H. D.; *Chemosphere* **2000**, *41*, 1193.
- Lee, J.-C.; Kim, M.-S.; Kim, B.-W.; *Water Res.* **2002**, *36*, 1776.
- Pucher, P.; Benmami, M.; Azouani, R.; Krammer, G.; Chhor, K.; Bocquet, J.-F.; Kanaev, A. V.; *Appl. Catal., A* **2007**, *332*, 297.
- Mascolo, G.; Comparelli, R.; Curri, M. L.; Lovecchio, G.; Lopez, A.; Agostiano, A.; *J. Hazard Mater.* **2007**, *142*, 130.
- Gao Y.; Liu, H.; *Mater. Chem. Phys.* **2005**, *92*, 604.
- Palominos, R. A.; Mondaca, M. A.; Giraldo, A.; Peñuela, G.; Pérez-Moya, M.; Mansilla, H. D.; *Catal. Today* **2009**, *144*, 100.
- Sakthivel, S.; Neppolian, B.; Shankar, M. V.; Arabindoo, B.; Palanichamy, M.; Murugesan, V.; *Sol. Energy Mater. Sol. Cells* **2003**, *77*, 65.
- Behnajady, M. A.; Modirshahla, N.; Daneshvar, N.; Rabbani, M.; *J. Hazard Mater.* **2007**, *140*, 257.
- Rodríguez-Couto, S.; Domínguez, A.; Sanromán, A.; *Chemosphere* **2002**, *46*, 83.
- Lawton, L. A.; Robertson, P. K. J.; Robertson, R. F.; Bruce, F. G.; *Appl. Catal., B* **2003**, *44*, 9.
- Yoon, S.-J.; Lee, Y. H.; Cho, W.-J.; Koh, I.-O.; Yoon, M.; *Catal. Commun.* **2007**, *8*, 1851.
- Yeber, M. C.; Freer, J.; Baeza, J.; Mansilla, H. D. in Proceedings of the *Second International Conference on Advanced Wastewater Treatment Recycling and Reuse*, Milan, Italy, 1998, p. 907.
- Zhao, S.; Xu, J.; Zhong, X. B.; *Catal. Today* **2004**, *93-95*, 857.
- Abellán, M. N.; Giménez, J.; Esplugas, S.; *Catal. Today* **2009**, *144*, 131.
- Kumar, S.; Dwevedi, A.; Kayastha, A. M.; *J. Mol. Catal. B: Enzym.* **2009**, *58*, 138.
- Bajpai S. K.; Sharma, S.; *React. Funct. Polym.* **2004**, *59*, 129.
- Gelover, S.; Mondragón, P.; Jiménez, A.; *J. Photochem. Photobiol., A* **2004**, *165*, 241.
- Gao X.; Wachs, I. E.; *Catal. Today* **1999**, *51*, 233.
- Choi, H. C.; Jung, Y. M.; Kim, S. B.; *Vib. Spectrosc.* **2005**, *37*, 33.
- Martínez, C.; Canle, M.; Fernández, M. I.; Santaballa, J. A.; Faria, J.; *Appl. Catal., B* **2011**, *102*, 563.

Submitted: December 23, 2011

Published online: August 7, 2012